

Electronic properties of the dimerized one-dimensional Hubbard model using lattice density-functional theory

R. López-Sandoval

*Instituto Potosino de Investigación Científica y Tecnológica,
Av. Venustiano Carranza 2425-A, 78210 San Luis Potosí, México*

G. M. Pastor

*Laboratoire de Physique Quantique, Université Paul Sabatier,
Centre National de la Recherche Scientifique,
118 route de Narbonne, 31062 Toulouse, France*

(Dated: November 2, 2018)

Abstract

The dimerized one-dimensional Hubbard model is studied in the framework of lattice density-functional theory (LDFT). The single-particle density matrix γ_{ij} with respect to the lattice sites is considered as basic variable. The corresponding interaction-energy functional $W[\gamma_{ij}]$ is defined by Levy's constrained search. Exact numerical results are obtained for $W(\gamma_{12}, \gamma_{23})$ where $\gamma_{12} = \gamma_{i,i+1}$ for i odd and $\gamma_{23} = \gamma_{i,i+1}$ for i even are the nearest-neighbor density-matrix elements along the chain. The domain of representability of γ_{ij} and the functional dependence of $W(\gamma_{12}, \gamma_{23})$ are analyzed. A simple, explicit approximation to $W(\gamma_{12}, \gamma_{23})$ is proposed, which is derived from scaling properties of W , exact dimer results, and known limits. Using this approximation, LDFT is applied to determine ground-state properties and charge-excitation gaps of finite and infinite dimerized chains as a function of the Coulomb-repulsion strength U/t and of the alternation δt of the hopping integrals t_{ij} ($t_{ij} = t \pm \delta t$). The accuracy of the method is demonstrated by comparison with available exact solutions and accurate numerical calculations. Goals and limitations of the present approach are discussed particularly concerning its ability to describe the crossover from weak to strong electron correlations.

PACS numbers: 71.15.Mb, 71.10.Fd

I. INTRODUCTION

Hohenberg and Kohn (HK) replaced the wave function by the electronic density $\rho(\vec{r})$ as the fundamental variable of the many-body problem and thereby achieved a crucial breakthrough in the theoretical description of the electronic properties of matter.¹ Since then, density functional theory (DFT) has been the subject of remarkable developments. Formal improvements, extensions, and uncountable successful applications to a large variety of problems have made of this theory the most efficient, albeit not infallible, method of determining physical and chemical properties of matter from first principles.^{2,3} Density functional (DF) calculations are usually based on the Kohn-Sham (KS) scheme which reduces the correlated N -particle problem to the solution of a set of self-consistent single-particle equations.⁴ While this transformation is formally exact, the form of the interaction-energy functional $W[\rho(\vec{r})]$ involved in the KS equations is not known explicitly. Practical implementations of DFT always require approximations to $W[\rho(\vec{r})]$, or equivalently to the exchange and correlation (XC) functional $E_{\text{XC}}[\rho(\vec{r})]$, on which the quality of the results depends crucially. Therefore, understanding the functional dependence of $W[\rho(\vec{r})]$ and exploring new ways of improving its approximations are central to the development of DF methods.

The most extensively used forms for $W[\rho(\vec{r})]$ are presently the local density approximation (LDA),⁴ its spin-polarized version or local spin-density approximation (LSDA)⁵ and the gradient corrected extensions,⁶ which were originally derived from exact results for the homogeneous electron gas. Despite an unparalleled success in the most diverse areas, the LDA-based approach fails systematically in accounting for phenomena that involve strong electron-correlation effects as observed, for example, in Mott insulators, heavy-fermion materials, or high- T_c superconductors. These systems are usually described in the framework of parametrized lattice Hamiltonians such as Anderson,⁷ Hubbard,⁸ Pariser-Parr-Pople,⁹ and related models which focus on the most relevant electron dynamics at low energies. However, even with simplified model interactions and a minimal number of orbitals per atom, a detailed understanding of the electronic properties in the strongly correlated limit remains a serious theoretical challenge. Exact results are rare or numerically very demanding and a variety elaborate many-body techniques have been specifically developed in order to study this problem.¹⁰ Being in principle an exact theory, the limitations of the DF approach have to be ascribed to the approximations used for exchange and correlation and not to the un-

derlying formalism. It is therefore very interesting to extend the range of applicability of DFT to the many-body lattice models that describe the physics of strongly correlated systems. Moreover, the development of lattice density-functional theory (LDFT) constitutes an intrinsically inhomogeneous approach and provides a true alternative to the LSDA and related gradient-corrected methods. Thus, studies on simple models can open new insights into the properties of W that should also be useful for future extensions to more realistic Hamiltonians and first principles calculations.

Several physical problems have been already investigated by applying the concepts of DFT to lattice models, for example, the band-gap problem in semiconductors,¹¹ the role of off-diagonal elements of the density matrix and the non-interacting v representability in strongly correlated systems,¹² or the development of energy functionals of the density matrix with applications to Hubbard and Anderson models.¹³ In previous works^{14,15} we have considered a density-matrix functional theory of many-body lattice models, that is analogous to Gilbert's approach in the continuum,¹⁶ and applied it to the Hubbard Hamiltonian with uniform nearest-neighbor (NN) hopping integrals $t_{ij} = t$. The interaction energy W of the Hubbard model has been calculated exactly as a function of the density matrix γ_{ij} for various periodic lattices having $\gamma_{ij} = \gamma_{12}$ for all nearest neighbors i and j . An analysis of the functional dependence of $W(\gamma_{12})$ for different band fillings and lattice structures revealed very interesting scaling properties.¹⁴ On this basis, a simple general approximation to $W(\gamma_{12})$ has been derived which yields a remarkable agreement with available exact results in 1D systems and which predicts successfully the ground-state energy and charge-excitation gap of the 2D Hubbard model in the complete range of interaction strength.¹⁵ This shows that DFT with an appropriate approximation to W is an efficient tool for determining the electronic properties of many-body lattice models.

The purpose of this paper is to extend the method by allowing for alternations of the density-matrix elements γ_{ij} between nearest neighbors in order to study the dimerized 1D Hubbard model. This problem has motivated a considerable research activity in past years, particularly concerning the role of electron correlations in the dimerization of polymer chains like polyacetylene.¹⁷ In this context two qualitatively different regimes may be distinguished depending on the relative importance of the intra-atomic Coulomb repulsion U and the NN hopping integral t . On the one side, for small U/t , the dimerization can be regarded as a bond-order wave that opens a gap at the Fermi surface of the one-dimensional (1D) single-

particle band-structure (Peierls distortion). On the other side, for large U/t , local charge fluctuations are severely reduced and the low-energy properties are dominated by antiferromagnetic (AF) correlations between spin degrees of freedom. In this case the dimerization can be regarded as an alternation of the strength of AF correlations along the chain or spin-Peierls state. One of our aims is to analyze the differences between these two types of behaviors in the framework of LDFT. The properties of dimerized chains are also very interesting from a purely methodological point of view. They provide in fact a simple, physically motivated means of exploring the functional dependence of $W[\gamma_{ij}]$ by including additional degrees of freedom, thereby allowing for a larger flexibility. Moreover, several exact results are available to compare with (e.g., Bethe-Ansatz solution for the non-dimerized Hubbard chain, finite-ring Lanczos diagonalizations, or density-matrix renormalization-group calculations) which allow to quantify the accuracy of the final results.

The remainder of the paper is organized as follows. In Sec. II the main steps in the formulation of LDFT are briefly recalled. The properties of the interaction-energy functional W of the dimerized Hubbard model are discussed in Sec. III. The domain of representability of γ_{ij} and the scaling behavior of W are investigated. A simple explicit approximation to W is derived, which is appropriate for direct calculations. Sec. IV is concerned with applications. The ground-state energy and the charge-excitation gap of finite and infinite dimerized chains are determined as a function of Coulomb-repulsion strength U/t and hopping-integral alternation δt . The LDFT results are contrasted with accurate numerical solutions in order to discuss goals and limitations of the present approach. Finally, Sec. V summarizes the main conclusions and points out some future perspectives.

II. DENSITY FUNCTIONAL THEORY ON A LATTICE

We consider the many-body Hamiltonian

$$H = \sum_{ij\sigma} t_{ij} \hat{c}_{i\sigma}^\dagger \hat{c}_{j\sigma} + \frac{1}{2} \sum_{\substack{klmn \\ \sigma\sigma'}} V_{klmn} \hat{c}_{k\sigma}^\dagger \hat{c}_{m\sigma'}^\dagger \hat{c}_{n\sigma'} \hat{c}_{l\sigma} , \quad (1)$$

where $\hat{c}_{i\sigma}^\dagger$ ($\hat{c}_{i\sigma}$) is the usual creation (annihilation) operator for an electron with spin σ at site or orbital i . The hopping integrals t_{ij} define the lattice (e.g., 1D chains, square or triangular 2D lattices) and the range of single-particle interactions (e.g., up to first or second neighbors). From the *ab initio* perspective t_{ij} is given by the external potential $V_{\text{ext}}(\vec{r})$ and by the choice

of the basis. V_{klmn} defines the type of many-body interactions which may be repulsive (Coulomb like) or attractive (in order to simulate electronic pairing) and which are usually approximated as short ranged (e.g., intra-atomic). Eq. (1) is mainly used in this section to present the general formulation which can then be applied to various specific models by simplifying the interactions. A particularly relevant example, to be considered in some detail in following sections, is the single-band Hubbard Hamiltonian with NN hoppings.⁸ The non-dimerized form of this model is obtained from Eq. (1) by setting $t_{ij} = -t$ for i and j NN's, $t_{ij} = 0$ otherwise, and $V_{klmn} = U\delta_{kl}\delta_{nm}\delta_{kn}$.

The hopping matrix t_{ij} plays the role given in conventional DFT to the external potential $V_{ext}(\vec{r})$. Consequently, the single-particle density matrix γ_{ij} between lattice sites replaces the continuum density $\rho(\vec{r})$ as basic variable. The situation is similar to the density-matrix functional theory proposed by Gilbert for the study of non-local pseudo-potentials $V_{ext}(\vec{r}, \vec{r}')$.^{16,18,19} The ground-state energy E_{gs} and density matrix γ_{ij}^{gs} are determined by minimizing the energy functional

$$E[\gamma_{ij}] = E_K[\gamma_{ij}] + W[\gamma_{ij}] \quad (2)$$

with respect to γ_{ij} . $E[\gamma_{ij}]$ is defined for all density matrices that can be written as

$$\gamma_{ij} = \sum_{\sigma} \gamma_{ij\sigma} = \sum_{\sigma} \langle \Psi | \hat{c}_{i\sigma}^{\dagger} \hat{c}_{j\sigma} | \Psi \rangle \quad (3)$$

for all i and j , where $|\Psi\rangle$ is an N -particle state. In other words, γ_{ij} derives from a physical state and is said to be pure-state N -representable.²⁰ The first term in Eq. (2) is given by

$$E_K = \sum_{ij} t_{ij} \gamma_{ij} . \quad (4)$$

It represents the kinetic energy associated with the electronic motion in the lattice and includes all single-particle contributions. Notice that Eq. (4) yields the exact kinetic energy and that no corrections on E_K have to be included in other parts of the energy functional as in the KS approach. The second term in Eq. (2) is the interaction-energy functional given by²¹

$$W[\gamma_{ij}] = \min \left[\frac{1}{2} \sum_{\substack{klmn \\ \sigma\sigma'}} V_{klmn} \langle \Psi[\gamma_{ij}] | \hat{c}_{k\sigma}^{\dagger} \hat{c}_{m\sigma'}^{\dagger} \hat{c}_{n\sigma'} \hat{c}_{l\sigma} | \Psi[\gamma_{ij}] \rangle \right] , \quad (5)$$

where the minimization implies a search over all N -particles states $|\Psi[\gamma_{ij}]\rangle$ that satisfy

$$\langle \Psi[\gamma_{ij}] | \sum_{\sigma} \hat{c}_{i\sigma}^{\dagger} \hat{c}_{j\sigma} | \Psi[\gamma_{ij}] \rangle = \gamma_{ij} \quad (6)$$

for all i and j . $W[\gamma_{ij}]$ represents the minimum value of the interaction energy compatible with a given density matrix γ_{ij} . It is often expressed in terms of the Hartree-Fock energy

$$E_{\text{HF}}[\gamma_{ij}] = \frac{1}{2} \sum_{\substack{ijkl \\ \sigma\sigma'}} V_{ijkl} (\gamma_{ij\sigma} \gamma_{kl\sigma'} - \delta_{\sigma\sigma'} \gamma_{il\sigma} \gamma_{kj\sigma}) \quad (7)$$

and the correlation energy $E_{\text{C}}[\gamma_{ij}]$ as

$$W[\gamma_{ij}] = E_{\text{HF}}[\gamma_{ij}] + E_{\text{C}}[\gamma_{ij}] . \quad (8)$$

W and E_{C} are universal functionals of γ_{ij} in the sense that they are independent of t_{ij} , i.e., of the system under study. They depend on the considered interactions or model, as defined by V_{klmn} , on the number of electrons N_e , and on the structure of the many-body Hilbert space, as given by N_e and the number of orbitals or sites N_a .

$E[\gamma]$ is minimized by expressing $\gamma_{ij} = \gamma_{ij\uparrow} + \gamma_{ij\downarrow}$ in terms of the eigenvalues $\eta_{k\sigma}$ (occupation numbers) and eigenvectors $u_{ik\sigma}$ (natural orbitals) as

$$\gamma_{ij\sigma} = \sum_k u_{ik\sigma} \eta_{k\sigma} u_{jk\sigma}^* . \quad (9)$$

Lagrange multipliers μ and $\lambda_{k\sigma}$ ($\varepsilon_{k\sigma} = \lambda_{k\sigma}/\eta_{k\sigma}$) are introduced in order to impose the usual constraints $\sum_{k\sigma} \eta_{k\sigma} = N_e$ and $\sum_i |u_{ik\sigma}|^2 = 1$. Derivation with respect to $u_{jk\sigma}^*$ and $\eta_{k\sigma}$ ($0 \leq \eta_{k\sigma} \leq 1$) yields the eigenvalue equations^{15,16}

$$\eta_{k\sigma} \sum_i \left(t_{ij} + \frac{\partial W}{\partial \gamma_{ij}} \right) u_{ik\sigma} = \varepsilon_{k\sigma} u_{jk\sigma} \quad (10)$$

with the following conditions relating $\eta_{k\sigma}$ and $\varepsilon_{k\sigma}$:

$$\varepsilon_{k\sigma} < \mu \quad \text{if} \quad \eta_{k\sigma} = 1 , \quad (11)$$

$$\varepsilon_{k\sigma} = \mu \quad \text{if} \quad 0 < \eta_{k\sigma} < 1 , \quad (12)$$

and

$$\varepsilon_{k\sigma} > \mu \quad \text{if} \quad \eta_{k\sigma} = 0 . \quad (13)$$

Self-consistency is implied by the dependence of $\partial W / \partial \gamma_{ij}$ on $\eta_{k\sigma}$ and $u_{ik\sigma}$. Eqs. (10)–(13) hold exactly in all interaction regimes. They are analogous to well-known results of density-matrix functional theory in the continuum.¹⁶ However, notice the difference with the KS-like approach considered in Ref.¹², which assumes non-interacting v -representability, and where only integer occupations are allowed.

The importance of fractional natural-orbital occupations has already been stressed in previous density-matrix functional studies in the continuum.¹⁶ In fact, in the case of models one observes that $0 < \eta_{k\sigma} < 1$ for all $k\sigma$ except in very special situations like the uncorrelated limit ($V_{klmn} = 0$) or the fully-polarized ferromagnetic state in the Hubbard model. This can be understood from perturbation-theory arguments —none of the $\eta_{k\sigma}$ should be a good quantum number for $V_{klmn} \neq 0$ — and has been explicitly demonstrated in exact solutions for finite systems or for the 1D Hubbard chain.²² Therefore, the case (12) is the only relevant one in general. All $\varepsilon_{k\sigma}$ in Eq. (10) must be degenerate or equivalently

$$t_{ij} + \partial W / \partial \gamma_{ij\sigma} = \delta_{ij} \mu . \quad (14)$$

Clearly, approximations of W in terms of the diagonal γ_{ii} alone can never yield such a behavior. Given a self-consistent scheme that implements the variational principle, the challenge remains to find good approximations to $W[\gamma_{ij}]$ that are simple enough to be applied in practical calculations.

III. INTERACTION-ENERGY FUNCTIONAL

In order to determine $W[\gamma_{ij}]$ from Eq. (5) we look for the extremes of

$$\begin{aligned} F = & \sum_{\substack{klmn \\ \sigma\sigma'}} \left[V_{klmn} \langle \Psi | \hat{c}_{k\sigma}^\dagger \hat{c}_{m\sigma'}^\dagger \hat{c}_{n\sigma} \hat{c}_{l\sigma} | \Psi \rangle \right] + \varepsilon \left(1 - \langle \Psi | \Psi \rangle \right) \\ & + \sum_{i,j} \lambda_{ij} \left(\langle \Psi | \sum_{\sigma} \hat{c}_{i\sigma}^\dagger \hat{c}_{j\sigma} | \Psi \rangle - \gamma_{ij} \right) \end{aligned} \quad (15)$$

with respect to $|\Psi\rangle$. Lagrange multipliers ε and λ_{ij} have been introduced to enforce the normalization of $|\Psi\rangle$ and the representability of γ_{ij} as required by Eq. (6). Derivation with respect to $\langle \Psi |$, ε and λ_{ij} yields the eigenvalue equations¹⁴

$$\sum_{ij\sigma} \lambda_{ij} \hat{c}_{i\sigma}^\dagger \hat{c}_{j\sigma} |\Psi\rangle + \sum_{\substack{klmn \\ \sigma\sigma'}} V_{klmn} \hat{c}_{k\sigma}^\dagger \hat{c}_{m\sigma'}^\dagger \hat{c}_{n\sigma} \hat{c}_{l\sigma} |\Psi\rangle = \varepsilon |\Psi\rangle , \quad (16)$$

and the auxiliary conditions $\langle \Psi | \Psi \rangle = 1$ and $\gamma_{ij} = \langle \Psi | \sum_{\sigma} \hat{c}_{i\sigma}^\dagger \hat{c}_{j\sigma} | \Psi \rangle$. The Lagrange multipliers λ_{ij} play the role of hopping integrals to be chosen in order that $|\Psi\rangle$ yields the given γ_{ij} . The pure-state representability of γ_{ij} ensures that there is always a solution. The subset of γ_{ij} that can be represented by a ground-state of Eq. (16) for some λ_{ij} is the physically relevant one, since it necessarily includes the absolute minimum γ_{ij}^{gs} of $E[\gamma_{ij}]$. Nevertheless, it should

be noted that pure-state representable γ_{ij} may be considered that can only be described by excited states or by linear combinations of eigenstates of Eq. (16).¹⁴

The general functional $W[\gamma_{ij}]$, valid for all lattice structures and for all types of hybridizations, can be simplified at the expense of universality if the hopping integrals are short ranged. For example, if only NN hoppings are considered, the kinetic energy E_K is independent of the density-matrix elements between sites that are not NN's. Therefore, the constrained search in Eq. (5) may be restricted to the $|\Psi[\gamma_{ij}]\rangle$ that satisfy Eq. (6) only for $i = j$ and for NN ij . This reduces significantly the number of variables in $W[\gamma_{ij}]$ and renders the determination and interpretation of the functional dependence far simpler.

In Sec. III A we present and discuss exact results for the interaction energy $W[\gamma_{ij}]$ of the dimerized Hubbard model on representative finite and infinite chains. These are obtained by solving Eq. (16) using accurate numerical methods. The dependence of the interaction energy on the alternating NN density-matrix elements γ_{12} and γ_{23} is analyzed. Scaling properties are identified within the domain of representability of γ_{ij} . On the basis of these results we propose, in Sec. III B, a simple general approximation to $W(\gamma_{12}, \gamma_{23})$ which is useful for practical applications. A first test on the accuracy of this approximation is also provided by comparison with available exact solutions.

A. Exact calculated $W[\gamma_{ij}]$ of the dimerized Hubbard model

In the following we consider the dimerized 1D Hubbard model which in the usual notation is given by⁸

$$H = \sum_{\langle ij \rangle \sigma} t_{ij} \hat{c}_{i\sigma}^\dagger \hat{c}_{j\sigma} + U \sum_i \hat{n}_{i\downarrow} \hat{n}_{i\uparrow}. \quad (17)$$

The NN hopping integrals t_{ij} take two alternating values: $t_{i,i+1} = t_{12} = t + \delta t$ for i odd and $t_{i,i+1} = t_{23} = t - \delta t$ for i even. The corresponding interaction-energy functional reads

$$W[\gamma_{ij}] = \min \left[U \sum_l \langle \Psi[\gamma_{ij}] | \hat{n}_{l\uparrow} \hat{n}_{l\downarrow} | \Psi[\gamma_{ij}] \rangle \right], \quad (18)$$

where the minimization is performed with respect to all N -particle states $|\Psi[\gamma_{ij}]\rangle$ satisfying $\langle \Psi[\gamma_{ij}] | \sum_\sigma \hat{c}_{i\sigma}^\dagger \hat{c}_{j\sigma} | \Psi[\gamma_{ij}] \rangle = \gamma_{ij}$ for NN ij . For repulsive interactions $W[\gamma_{ij}]$ represents the minimum average number of double occupations corresponding to a given degree of electron

delocalization, i.e., to a given γ_{ij} . Eq. (16) then reduces to

$$\sum_{\substack{\langle ij \rangle \\ \sigma}} \lambda_{ij} \hat{c}_{i\sigma}^\dagger \hat{c}_{j\sigma} |\Psi\rangle + U \sum_i \hat{n}_{i\uparrow} \hat{n}_{i\downarrow} |\Psi\rangle = \varepsilon |\Psi\rangle. \quad (19)$$

This eigenvalue problem can be solved numerically for finite systems with various boundary conditions. To this aim we expand $|\Psi[\gamma_{ij}]\rangle$ in a complete set of basis states $|\Phi_m\rangle$ which have definite occupation numbers $\nu_{i\sigma}^m$ at all orbitals $i\sigma$: $\hat{n}_{i\sigma}|\Phi_m\rangle = \nu_{i\sigma}^m|\Phi_m\rangle$ with $\nu_{i\sigma}^m = 0$ or 1 . The values of $\nu_{i\sigma}^m$ satisfy the usual conservation of the number of electrons $N_e = N_{e\uparrow} + N_{e\downarrow}$ and of the z component of the total spin $S_z = (N_{e\uparrow} - N_{e\downarrow})/2$, where $N_{e\sigma} = \sum_i \nu_{i\sigma}^m$. For not too large clusters, the state $|\Psi_0[\gamma_{ij}]\rangle$ corresponding to the minimum in Eq. (18) —the ground state of Eq. (19)— can be determined by sparse-matrix diagonalization procedures such as the Lanczos iterative method.²³ For large chains, the properties of $|\Psi_0[\gamma_{ij}]\rangle$ can be calculated using the density-matrix renormalization-group (DMRG) method²⁴ which allows reliable extrapolations to the infinite-length limit. Finally, in the absence of dimerization ($\delta t = 0$) translational symmetry implies that all NN γ_{ij} are the same, and therefore one may set $\lambda_{ij} = \lambda$ for all NN ij . The lowest eigenvalue of Eq. (19) can then be determined from Lieb and Wu's exact solution of the 1D Hubbard model following the work by Shiba.²²

In Fig. 1 the interaction energy W of dimerized Hubbard chains is shown in the form of constant-energy curves given by $W(\gamma_{12}, \gamma_{23}) = \lambda E_{\text{HF}}$, where $\gamma_{12} = \gamma_{i,i+1}$ for i odd and $\gamma_{23} = \gamma_{i,i+1}$ for i even are the density-matrix elements or bond orders between NN's. $E_{\text{HF}} = U/4$ stands for the Hartree-Fock energy, and λ is a constant ($0 \leq \lambda \leq 1$). Results are presented for the $N_a = 12$ site ring and for the infinite 1D chain which were obtained from Eq. (19) by using Lanczos-diagonalization and DMRG methods, respectively.^{23,24} Only positive γ_{12} and γ_{23} are considered since this is the relevant domain when all the hopping integrals have the same sign. In bipartite lattices, like open chains or rings with even N_a , the sign of the NN bond orders can be changed without altering W by changing the sign of the local orbitals at one of the sublattices. Thus, $W(\gamma_{12}, \gamma_{23}) = W(-\gamma_{12}, -\gamma_{23})$. Moreover, $W(\gamma_{12}, \gamma_{23}) = W(\gamma_{23}, \gamma_{12})$ as even an odd sites can be interchanged by a simple translation (N_a even for rings).

The domain of definition of W is restricted by the pure-state representability of γ_{ij} . The axes $\gamma_{12} = 0$ and $\gamma_{23} = 0$ in Fig. 1 represent a collection of disconnected dimers or fully dimerized states, while $\gamma_{12} = \gamma_{23}$ corresponds to non-dimerized states. In between, the degree of dimerization can be measured by the angle $\phi = \arctan(\gamma_{12}/\gamma_{23})$. The degree of

electron delocalization for each ϕ is characterized by $\gamma = \sqrt{\gamma_{12}^2 + \gamma_{23}^2}$, which is bounded by $\gamma^\infty(\phi) \leq \gamma \leq \gamma^0(\phi)$ in order that γ_{ij} remains pure-state representable. The density-matrix elements along the curve $\gamma = \gamma^0(\phi)$ are the largest bond orders that can be achieved on a given lattice and for given N_a and N_e [$(\gamma_{12}^0, \gamma_{23}^0) = \gamma^0(\phi)(\cos \phi, \sin \phi)$]. They represent the maximum electron delocalization for each ϕ and yield the extremes of the kinetic energy $E_K = \sum t_{ij} \gamma_{ij}$, with different ϕ corresponding to different t_{12}/t_{23} . Thus, for $\gamma = \gamma^0(\phi)$ the density matrix can be represented by the ground state of the uncorrelated Hubbard model for some t_{12}/t_{23} ($U = 0$). In the absence of degeneracy the underlying electronic state $|\Psi_0\rangle$ is a single Slater determinant and $W(\gamma_{12}^0, \gamma_{23}^0) = E_{\text{HF}}$. Consequently, the upper bound for γ coincides with the $\lambda = 1$ curve in Fig. 1. The correlation energy $E_C = W - E_{\text{HF}}$ vanishes as expected in the fully delocalized limit. For $U = 0$ the minimization of the energy $E = E_K$ as a function of γ_{ij} can be stated in terms of the representability of γ_{ij} alone. In this case the equilibrium condition yielding γ_{ij}^{gs} is achieved at the borders of the domain of representability, more precisely, when the normal to the curve $\gamma = \gamma^0(\phi)$ is parallel to $\vec{\nabla} E_K = (t_{12}, t_{23})$.

Concerning the lower bound $\gamma^\infty(\phi)$, one should first note that as γ decreases, $\gamma < \gamma^0(\phi)$, it is possible to construct correlated states $|\Psi[\gamma_{ij}]\rangle$ having increasingly localized electrons. Charge fluctuations can then be reduced more efficiently for smaller γ , and therefore the Coulomb interaction energy decreases with decreasing γ [see Eq. (18) and Fig. 1]. W reaches its minimum value $W_\infty = U \max\{0, N_e - N_a\}$ in the strongly correlated limit where $\gamma = \gamma^\infty(\phi)$. For half-band filling this corresponds to a fully localized state having $\gamma^\infty(\phi) = 0$ and $W_\infty = 0$. However, note that for $N_e \neq N_a$, W reaches W_∞ already for $\gamma^\infty(\phi) > 0$ since partially delocalized states can be found having minimal Coulomb repulsion. This is the case for example in a fully-polarized ferromagnetic state.

Fig. 1 also provides a qualitative picture of the functional dependence of W for dimerized chains. On the one side, for strongly dimerized states ($\phi \simeq 0$ or $\phi \simeq \pi/2$) the constant- W curves resemble circumference arcs, the gradient $\vec{\nabla} W$ being approximately radial. This type of behavior is most clearly seen for weak or moderate correlations ($\lambda \geq 0.3$), while in the localized regime ($\lambda \leq 0.1$) it holds only for a very limited range of ϕ around $\phi = 0$ or $\phi = \pi/2$. On the other side, for weakly to moderately dimerized states ($\phi \simeq \pi/8 - \pi/4$) the level curves can be regarded in first approximation as straight lines parallel to $\gamma_{12} = -\gamma_{23}$. The very weak dependence of $\vec{\nabla} W$ on ϕ implies that for $\phi \simeq \pi/4$ the ground-

state values of γ_{12}^{gs} and γ_{23}^{gs} , which result from the minimization of $E = E_K + W$, are very sensitive to the hopping alternation δt . In fact, significant variations of ϕ are necessary until $\vec{\nabla}W = -\vec{\nabla}E_K \propto (1 + \delta t/t, 1 - \delta t/t)$ even for $\delta t/t \ll 1$. This is particularly notable for weak correlations since the $W = E_{\text{HF}}$ curve is strictly linear for $|\phi - \pi/4| < 0.05$. Therefore, a discontinuous change from $\gamma_{12}^{gs}/\gamma_{23}^{gs} = 1$ to $\gamma_{12}^{gs}/\gamma_{23}^{gs} = 0.91$ is found at $U = 0$ and arbitrary small δt . For $U > 0$, γ_{12}^{gs} and γ_{23}^{gs} are continuous functions of δt , although the dependence on δt remains very strong for small δt , as can be inferred from the level curves in the figure. Comparing subfigures (a) and (b) one observes that the results for $N_a = 12$ and $N_a = \infty$ are quite similar. The rather rapid convergence with chain length suggests that $W(\gamma_{12}, \gamma_{23})$ is not very sensitive to the details of the considered system, even if the minimization constraints in Eq. (18) apply only to NN bond orders. This is of interest for practical applications, as it will be discussed below.

In Fig. 2 the interaction energy W is shown as a function of γ for representative values of ϕ , including in particular the fully-dimerized ($\phi = 0$) and non-dimerized ($\phi = \pi/4$) cases. Despite the quantitative differences among the various ϕ , several qualitative properties are shared by all the curves: (i) As already discussed, the domain of representability of γ is bound for each ϕ by the bond order $\gamma^0(\phi)$ in the uncorrelated limit. γ^0 decreases monotonously with increasing ϕ for $0 \leq \phi \leq \pi/4$ showing that a compromise between γ_{12} and γ_{23} is made when the two bonds are active. This is an important contribution to the ϕ -dependence of W . (ii) In the delocalized limit, $W(\gamma^0, \phi) = E_{\text{HF}} = U/4$ for all ϕ , since the electronic state yielding the largest γ is a single Slater determinant. Moreover, one observes that $\partial W/\partial \gamma$ diverges at $\gamma = \gamma^0$ for all ϕ . This is a necessary condition in order that the ground-state density matrix satisfies $\gamma^{gs} < \gamma^0$ for arbitrary small $U > 0$, as expected from perturbation theory. (iii) Starting from $\gamma = \gamma^0$, W decreases with decreasing γ reaching its lowest possible value $W = 0$ for $\gamma = 0$ ($N_e = N_a$). The decrease of W with decreasing γ means that the reduction of the Coulomb energy due to correlations is done at the expense of kinetic energy or electron delocalization. (iv) In the limit of small γ one observes that $W \propto \gamma^2$. Therefore, for $U/t \gg 1$, $\gamma^{gs} \propto t/U$ and $E_{gs} \propto t^2/U$, a well known result in the Heisenberg limit of the half-filled Hubbard model.¹⁰

B. Scaling approximation to $W[\gamma_{ij}]$

In order to compare the γ -dependence of W for different ϕ and to analyze its scaling behavior it is useful to bring the domains of representability for different ϕ to a common range by considering $W(\gamma, \phi)$ as a function of $\gamma/\gamma^0(\phi)$, as displayed in Fig. 3. In this form the results for different ϕ appear as remarkably similar, showing that the largest part of the dependence of W on the ratio γ_{12}/γ_{23} comes from the domain of representability of γ_{ij} given by its upper bound $\gamma^0(\phi)$ [$\gamma^\infty(\phi) = 0$ for half-band filling]. An analogous scaling behavior has been found in previous numerical studies of $W(\gamma_{12})$ of non-dimerized Hubbard models, where γ_{12} refers to the NN density-matrix element.¹⁴ In this case one observes that $W(\gamma_{12})$ depends weakly on system size N_a , band-filling $n = N_e/N_a$, and lattice structure, if W is measured in units of the Hartree-Fock energy E_{HF} and if γ_{12} is scaled within the relevant domain of representability $[\gamma_{12}^\infty, \gamma_{12}^0]$. In the present context, Fig. 3 implies that the change in W associated to a given change in the degree of delocalization $\gamma/\gamma^0(\phi)$ can be regarded as nearly independent of ϕ and system size. A good general approximation to $W(\gamma, \phi)$ can then be obtained by applying such a scaling to the functional dependence extracted from a simple reference system. An appropriate choice is provided by the fully-dimerized chain corresponding to $\phi = 0$, which can be worked out analytically. In this case the system consists of a collection of dimers and the exact interaction energy reads

$$W(\gamma, \phi=0) = \frac{UN_a}{4} \left(1 - \sqrt{1 - \gamma^2} \right). \quad (20)$$

Scaling the functional dependence of the dimer interaction energy to the ϕ -dependent domain of representability one obtains

$$W_0(\gamma, \phi) = \frac{UN_a}{4} \left(1 - \sqrt{1 - \left[\frac{\gamma}{\gamma^0(\phi)} \right]^2} \right), \quad (21)$$

which we propose as approximation to W for dimerized systems. Notice that $W_0(\gamma, \phi)$ preserves the previous general properties (i)–(iv) and that it is of course exact for $\phi = 0$ [$\gamma^0(\phi=0) = 1$]. In practice, the system specific function $\gamma^0(\phi)$ can be easily obtained by integration of the single-particle spectrum.

It is important to remark that the density matrices γ_{ij} involved in the approximate functional W_0 are pure-state N -representable. Eq. (21) applies to the γ_{ij} obtained by scaling the off-diagonal elements of the density matrices γ_{ij}^0 that derive from uncorrelated states

$|\Psi_0\rangle$ having N_e electrons on N_a sites, and a uniform density distribution $\langle\Psi_0|\sum_\sigma\hat{n}_{i\sigma}|\Psi_0\rangle = N_e/N_a = 1$. In other terms, γ_{ij} has the form $\gamma_{ij} = \lambda\gamma_{ij}^0$ with $0 \leq \lambda \leq 1$ for all $i \neq j$, and $\gamma_{ii} = \gamma_{ii}^0 = 1$ for all i . In order to show the pure-state representability of γ_{ij} , we consider two normalized N -particles states $|\Psi_a\rangle$ and $|\Psi_b\rangle$ satisfying $\langle\Psi_a|\sum_\sigma\hat{c}_{i\sigma}^\dagger\hat{c}_{j\sigma}|\Psi_b\rangle = 0$ for all ij . This condition is fulfilled, for example, by states a and b having different defined total spins S or S_z , or by superpositions of pure- S or pure- S_z states sharing no common eigenvalues. The density-matrix represented by $|\Psi\rangle = \alpha|\Psi_a\rangle + \beta|\Psi_b\rangle$ with $\alpha^2 + \beta^2 = 1$ is then given by $\gamma_{ij} = \langle\Psi|\sum_\sigma\hat{c}_{i\sigma}^\dagger\hat{c}_{j\sigma}|\Psi\rangle = \alpha^2\gamma_{ij}^a + \beta^2\gamma_{ij}^b$, where γ_{ij}^a and γ_{ij}^b are the density matrices corresponding to $|\Psi_a\rangle$ and $|\Psi_b\rangle$. Therefore, all the density matrices in the segment defined by γ_{ij}^a and γ_{ij}^b are pure-state N -representable. The representability of a scaled uncorrelated γ_{ij}^0 at half-band filling follows from the previous lemma by taking $|\Psi_a\rangle = |\Psi_0\rangle$, which has $S = 0$ or $1/2$, and $|\Psi_b\rangle$ equal to the fully localized state with one electron per site and maximal $S = N_e/2$, for which $\gamma_{ij}^b = 0$ for all $i \neq j$, and $\gamma_{ii}^b = 1$ for all i . Consequently, the γ_{ij} in the domain of definition of W_0 and the ground-state density matrices γ_{ij}^{gs} derived from it are all pure-state N -representable.

Fig. 4 compares Eq. (21) with the exact $W(\gamma, \phi)$ for a 12-site Hubbard ring and for the infinite chain. One observes that the proposed approximation follows rather closely the exact results for all γ and ϕ . The largest discrepancies are found for vanishing or moderate dimerization (e.g., $\phi = 3\pi/16$ or $\phi = \pi/4$) and relatively large γ ($\gamma \simeq 0.8$). In all cases the quantitative differences remain small ($|W_0 - W|/U \leq 0.047$ for $\phi = \pi/4$ and $|W_0 - W|/U \leq 0.045$ for $\phi = 3\pi/8$) which is quite remarkable taking into account the simplicity of the approximation. In the following, Eq. (21) is applied in the framework of LDFT to determine several properties of the dimerized 1D Hubbard model. Comparison is made with exact results whenever possible in order to assess the performance of the method.

IV. DIMERIZED HUBBARD CHAINS

In Figs. 5 and 6 the ground-state energy E_{gs} , kinetic energy E_K , and Coulomb energy E_C of the 1D Hubbard model are given as a function of the Coulomb repulsion strength U/t for different hopping alternations δt . Accurate numerical results are also shown which were obtained using the Lanczos diagonalization method²³ for $N_a = 12$ or the DMRG method²⁴ for the infinite chain. In the case of the non-dimerized infinite chain, Lieb and Wu's exact

solution²² is taken as reference. The results for $N_a = 12$ and $N_a = \infty$ are qualitative very similar. E_{gs} increases monotonically with U/t since $\partial E_{gs}/\partial U = \langle \hat{n}_{i\uparrow}\hat{n}_{i\downarrow} \rangle > 0$, vanishing in the limit of $U/t = \infty$. For $U/t < 4$ this is essentially a consequence of the increase of $E_C \propto U$, as E_K and γ_{ij} remain very much like in the uncorrelated $U = 0$ state. In contrast, for $U/t > 4$ the electrons become increasingly localized, and the increase of E_{gs} results from the increase of E_K which approaches zero as $|\gamma_{ij}|$ decreases. At the same time E_C tends to zero as charge fluctuations are suppressed (see Figs. 5 and 6).

Comparison between LDFT and the exact results shows a very good agreement. This concerns not only E_{gs} but also the separate kinetic and Coulomb contributions indicating that electron localization and intra-atomic correlations are correctly described for all U/t . Moreover, this also shows that the results obtained for the ground-state energy are not the consequence of strong compensations of errors. Concerning the accuracy of E_K and E_C one generally observes that a somewhat higher precision is achieved for E_K , which functional dependence is known exactly, as compared to E_C , which derives from an approximation to W [Eq. (21)]. For $\delta t/t \geq 0.1$ the LDFT calculations are nearly indistinguishable from the exact ones (e.g., $|E_{gs} - E_{gs}^{ex}|/t \leq 0.03$ for $\delta t/t = 0.1$). Even the largest quantitative discrepancies, found for the non-dimerized chain at intermediate U/t , are pretty small. For instance, for $\delta t = 0$ and $U/t = 4$ we obtain $|E_{gs} - E_{gs}^{ex}|/t = 0.020$ for the 12-site ring and $|E_{gs} - E_{gs}^{ex}|/t = 0.044$ for the infinite chain. Comparing Figs. 5 and 6 one observes that the performance of the method is sometimes higher for the 12-site ring than for the infinite chain. For example, Fig. 6 shows that E_K (E_C) is slightly overestimated (underestimated) for $\delta t = 0$ and $U/(U + 4t) = 0.7\text{--}0.8$, whereas for $N_a = 12$ a much better agreement with the exact result is found (see Fig. 5). In any case it is important to recall that no artificial symmetry breaking is required to describe correlation-induced localization correctly, as it often occurs in other approaches (e.g., mean-field spin-density-wave state). Moreover, the present calculations remain simple and numerically not demanding, since the minimization of $E[\gamma_{ij}]$ is performed using analytical expressions for E_K and W [see Eqs. (4) and (21)]. One concludes that LDFT, combined with Eq. (21) as approximation to the interaction energy functional, provides an efficient and correct description of the ground-state properties of the 1D Hubbard model in the complete range of interaction strength and dimerization.

The charge-excitation or band gap

$$\Delta E_c = E_{gs}(N_e + 1) + E_{gs}(N_e - 1) - 2E_{gs}(N_e) \quad (22)$$

is a property of considerable interest in strongly correlated systems which can be related to the discontinuity in the derivative of the kinetic and correlation energies per site with respect to the electron density n . The determination of ΔE_c constitutes a much more serious challenge than the calculation of ground-state properties like E_{gs} , E_K , and E_C particularly in the framework of a density-functional formalism. Results for ΔE_c of the 1D Hubbard model are given in Figs. 7 and 8 as a function of the Coulomb repulsion strength U/t for different values of the hopping alternation δt ($n = 1$). ΔE_c vanishes for $\delta t = 0$ and $U/t = 0$, and increases with increasing U/t or δt . Comparison between LDFT and Lanczos exact diagonalizations ($N_a = 12$) or the Bethe-Ansatz solution²² ($N_a = \infty$ and $\delta t = 0$) shows fairly small quantitative discrepancies. In the most difficult non-dimerized case we find $|\Delta E_c - \Delta E_c^{ex}| < 0.18t$ for $N_a = 12$, and $|\Delta E_c - \Delta E_c^{ex}| < 0.34t$ for $N_a = \infty$. For small U/t and $\delta t = 0$, ΔE_c is somewhat underestimated for $N_a = 12$ and overestimated for $N_a = \infty$. The latter is mainly due to the fact that Eq. (21) fails to reproduce the exponential decrease of ΔE_c for $U/t \rightarrow 0$ ($N_a = \infty$ and $\delta t = 0$).²² As in previous properties the accuracy improves with increasing δt . Fig. 7 shows that the LDFT results for non-vanishing dimerization and $N_a = 12$ are very close to the exact ones ($|\Delta E_c - \Delta E_c^{ex}|/t < 0.011$ already for $\delta t/t = 0.1$). Therefore, one expects that the predictions for $N_a = \infty$ and $\delta t > 0$ should be reliable. Finally, one may note that in the limit of large U/t , the hopping alternation δt has little effect on the charge gap. As the electrons tend to localize for $U/t \rightarrow \infty$, $\Delta E_c \rightarrow U + E_b$ where $E_b = -4t$ is the energy of the bottom of the single-particle band. The present lattice-density-functional scheme describes correctly the crossover from a band insulator to a Mott insulator which occurs in dimerized chains as U/t is varied from the weak-interaction to the strong-interaction regime.

V. SUMMARY AND OUTLOOK

A novel density-functional approach to lattice-fermion models has been applied to the dimerized 1D Hubbard Hamiltonian. In this framework the basic variable is the single-particle density matrix γ_{ij} and the key unknown is the interaction-energy functional

$W[\gamma_{ij}]$. In the present paper we have first investigated the functional dependence of W on the density-matrix elements γ_{12} and γ_{23} between nearest neighbors in dimerized chains ($\gamma_{i,i+1} = \gamma_{12}$ for i odd and $\gamma_{i,i+1} = \gamma_{23}$ for i even). Rigorous results for $W(\gamma_{12}, \gamma_{23})$ were derived from finite-ring Lanczos diagonalizations and from DMRG calculations for the infinite chain. An analysis of these exact results shows that W can be appropriately scaled as a function $\gamma/\gamma^0(\phi)$, where $\gamma = \sqrt{\gamma_{12}^2 + \gamma_{23}^2}$ and $\gamma^0(\phi)$ is the largest representable γ for a given $\phi = \arctan(\gamma_{12}/\gamma_{23})$. A simple general approximation to W was then proposed which takes advantage of this scaling behavior and which provides with a unified description of correlations from weak to strong coupling regimes. Finally, using this approximation, several ground-state properties and the charge-excitation gap of dimerized chains have been determined successfully as a function of Coulomb repulsion strength U/t and hopping alternation δt .

The accuracy of the results encourages more or less straightforward applications of the present approach to related problems such as multi-leg ladders or the two-dimensional square lattice with first and second NN hoppings (t - t' Hubbard model). Moreover, the possibility of generalizing the present scaling approximation to an arbitrary number of independent variables γ_{ij} deserves to be investigated in detail, since it would open the way to applications in very low symmetry situations including metal clusters and disordered systems.

Acknowledgments

Helpful discussions with Dr. Ph. Maurel are gratefully acknowledged. This work has been supported by CONACyT (Mexico) through the project W-8001 (Millennium initiative). Computer resources were provided by IDRIS (CNRS, France).

¹ P. Hohenberg and W. Kohn, Phys. Rev. **136**, B864 (1964).

² R.G. Parr and W. Yang, *Density-Functional Theory of Atoms and Molecules* (Clarendon, Oxford, 1989);

³ R.M. Dreizler and E.K.U. Gross, *Density Functional Theory* (Springer, Berlin, 1990) and references therein.

⁴ W. Kohn and L.J. Sham, Phys. Rev. **140**, A1133 (1965).

- ⁵ U. von Barth and L. Hedin, J. Phys. C: Solid State Phys. **5**, 1629 (1972).
- ⁶ D.C. Langreth and M.J. Mehl, Phys. Rev. B **28**, 1809 (1983); A.D. Becke, Phys. Rev. A **38**, 3098 (1988); J.P. Perdew, K. Burke, and M. Ernzerhof, Phys. Rev. Lett. **77**, 3865 (1996), and references therein.
- ⁷ P.W. Anderson, Phys. Rev. **124**, 41 (1961).
- ⁸ J. Hubbard, Proc. R. Soc. London **A276**, 238 (1963); **A281**, 401 (1964); J. Kanamori, Prog. Theo. Phys. **30**, 275 (1963); M.C. Gutzwiller, Phys. Rev. Lett. **10**, 159 (1963).
- ⁹ R. Pariser and R.G. Parr, J. Chem. Phys. **21**, 466 (1953); *ibid.* 767 (1953); J. A. Pople, Trans. Faraday Soc. **49**, 1375 (1953).
- ¹⁰ See, for instance, P. Fulde, *Electron Correlations in Molecules and Solids* (Springer, Berlin, 1991).
- ¹¹ O. Gunnarsson and K. Schönhammer, Phys. Rev. Lett. **56**, 1968 (1986); A. Svane and O. Gunnarsson, Phys. Rev. B **37**, 9919 (1988); K. Schönhammer, O. Gunnarsson, and R.M. Noack, *ibid.* **52**, 2504 (1995).
- ¹² A. Schindlmayr and R.W. Godby, Phys. Rev. B **51**, 10427 (1995).
- ¹³ A.E. Carlsson, Phys. Rev. B **56**, 12058 (1997); R. G. Hennig and A. E. Carlsson, *ibid* **63**, 115116 (2001).
- ¹⁴ R. López-Sandoval and G.M. Pastor, Phys. Rev. B **61**, 1764 (2000).
- ¹⁵ R. López-Sandoval and G.M. Pastor, Phys. Rev. B (2002), in press. cond-mat/0207429.
- ¹⁶ T.L. Gilbert, Phys. Rev. B **12**, 2111 (1975).
- ¹⁷ See, for instance, H.C. Longuet-Higgins and L. Salem, Proc. Roy. Soc. **A 25**, 172 (1959); W.P. Su, J.R. Schrieffer, and A.J. Heeger, Phys. Rev. Lett. **42**, 1698 (1979); A. Karpfen and J. Petkov, Solid State Commun. **29**, 251 (1979); C.S. Yannoni and T.C. Clarke, Phys. Rev. Lett. **51**, 1191 (1983); S. Suhai, Chem. Phys. Lett. **96**, 619 (1983); M. Takahashi and J. Paldus, Int. J. Quantum Chem. **28**, 459 (1985); H. Kahlert, O. Leitner, and G. Leising, Synth. Met. **17**, 467 (1987); C.M. Liegener, J. Chem. Phys. **88**, 6999 (1988); J. Ashkenazi, W.E. Pickett, H. Krakauer, C.S. Wang, B.M. Klein, and S.R. Chubb, Phys. Rev. Lett. **62** 2016 (1989); G. König and G. Stollhoff, Phys. Rev. Lett. **65**, 1239 (1990); J.Q. Sun and R. J. Bartlett, J. Chem. Phys. **104** 8553 (1996); M.B. Lepetit and G.M. Pastor, Phys. Rev. B **56**, 4447 (1997); G.L. Bendazzoli, S. Evangelisti, G. Fano, F. Ortolani, and L. Ziosi, J. Chem. Phys. **110**, 1277 (1999).
- ¹⁸ R.A. Donnelly and R.G. Parr, J. Chem. Phys. **69**, 4431 (1978); R.A. Donnelly, *ibid.* **71**, 28744

- (1979). See also, Ref.², p. 213ff, and references therein.
- ¹⁹ S.M. Valone, J. Chem. Phys. **73**, 1344 (1980); *ibid.* 4653.
- ²⁰ An extension of the definition domain of $E[\gamma_{ij}]$ to ensemble-representable density matrices Γ_{ij} is straightforward following the work by Valone (see Ref.¹⁹). Ensemble density-matrices are written as $\Gamma_{ij} = \sum_n w_n \langle \Psi_n | \sum_\sigma \hat{c}_{i\sigma}^\dagger \hat{c}_{j\sigma} | \Psi_n \rangle$ with $w_n \geq 0$ and $\sum_n w_n = 1$. In practice, they are much easier to characterize than pure-state density matrices.
- ²¹ M. Levy, Proc. Natl. Acad. Sci. U.S.A. **76**, 6062 (1979).
- ²² L.H. Lieb and F.Y. Wu, Phys. Rev. Lett. **20**, 1445 (1968); H. Shiba, Phys. Rev. B **6**, 930 (1972).
- ²³ C. Lanczos, J. Res. Nat. Bur. Stand. **45**, 255 (1950); B.N. Parlett, *The Symmetric Eigenvalue Problem*, (Prentice-Hall, Engelwood Cliffs, NJ, 1980); J.K. Collum and R.A. Willoughby, *Lanczos Algorithms for Large Symmetric Eigenvalue Computations*, (Birkhauser, Boston, 1985), Vol. I.
- ²⁴ S.R. White, Phys. Rev. Lett. **69**, 2863 (1992); Phys. Rev. B **48**, 10345 (1993).

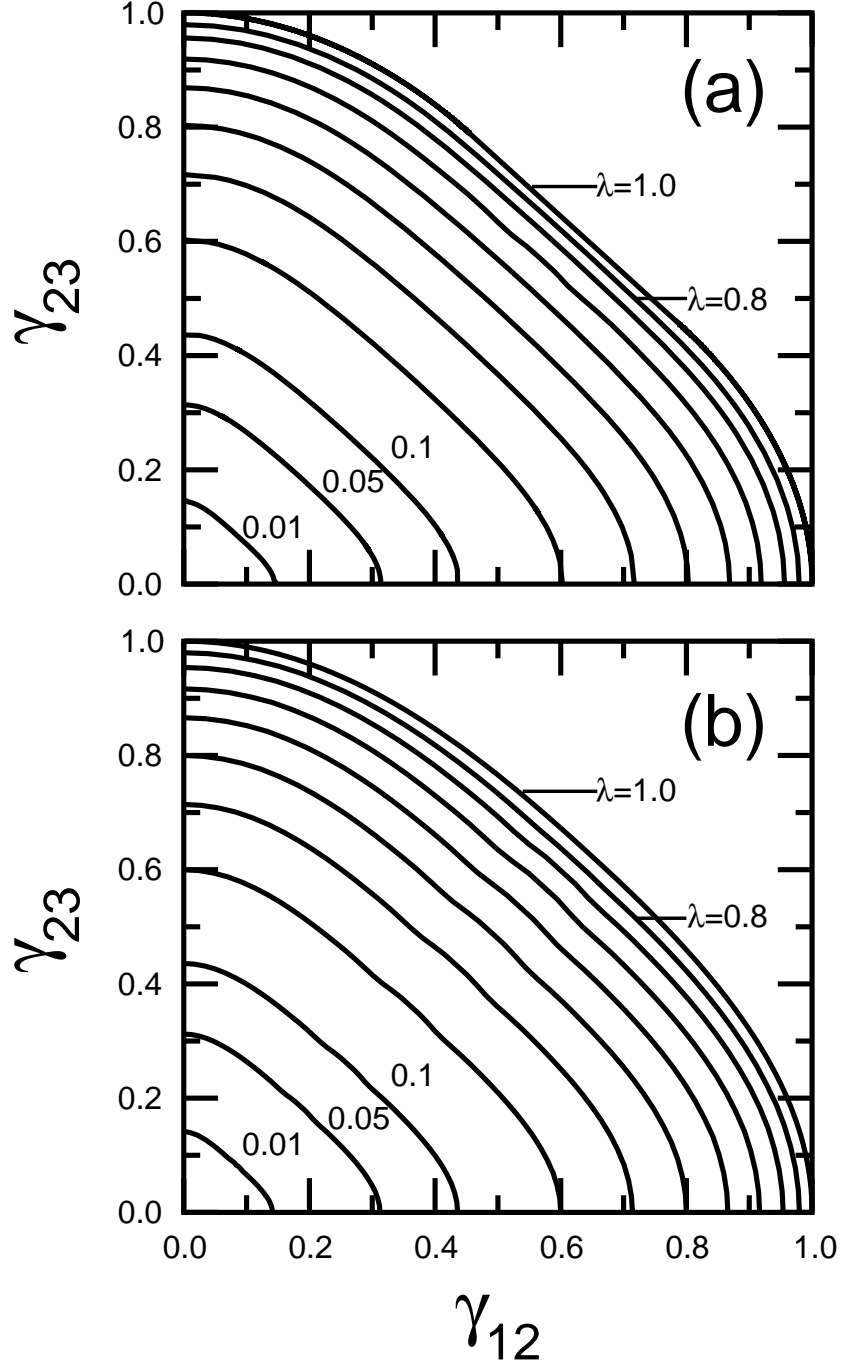


FIG. 1: Constant interaction-energy curves of the one-dimensional (1D) Hubbard model as given by $W(\gamma_{12}, \gamma_{23}) = \lambda E_{\text{HF}}$, where $E_{\text{HF}} = U/4$ is the Hartree-Fock energy and λ a constant ($0 \leq \lambda \leq 1$). The NN density-matrix elements are $\gamma_{i,i+1} = \gamma_{12}$ for i odd, and $\gamma_{i,i+1} = \gamma_{23}$ for i even. Results are given for (a) the $N_a = 12$ site ring and (b) the infinite chain, both at half-band filling ($N_e = N_a$). $\lambda = 1$ corresponds to uncorrelated states and defines the limit of representability of γ_{ij} . Unless indicated the difference in λ between contiguous curves is $\Delta\lambda = 0.1$.

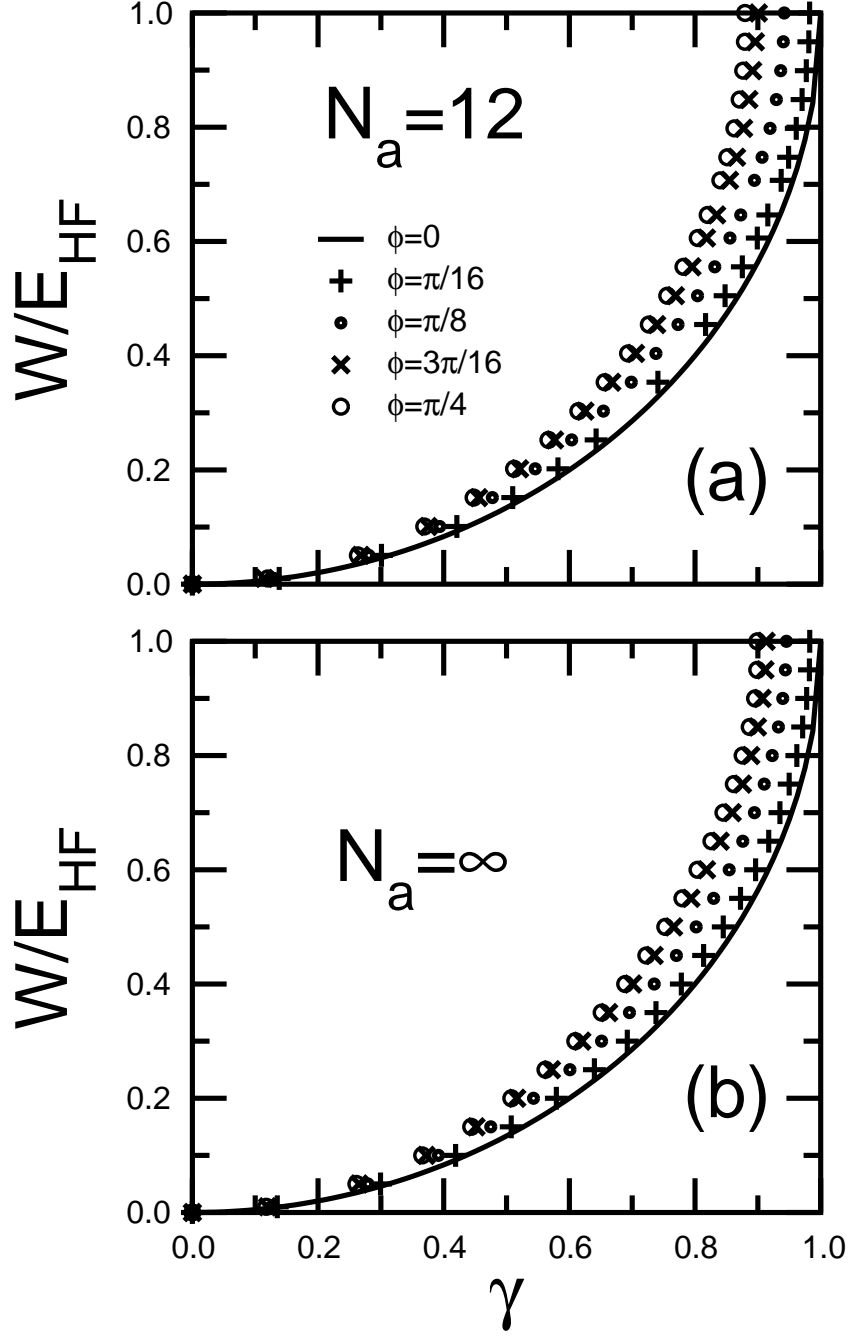


FIG. 2: Interaction-energy W of the 1D Hubbard model at half-band filling ($N_e = N_a$) as a function of $\gamma = \sqrt{\gamma_{12}^2 + \gamma_{23}^2}$ for different values of $\phi = \arctan(\gamma_{12}/\gamma_{23})$: (a) ring with $N_a = 12$ sites (b) infinite chain. The density-matrix elements are $\gamma_{i,i+1} = \gamma_{12}$ for i odd, and $\gamma_{i,i+1} = \gamma_{23}$ for i even.

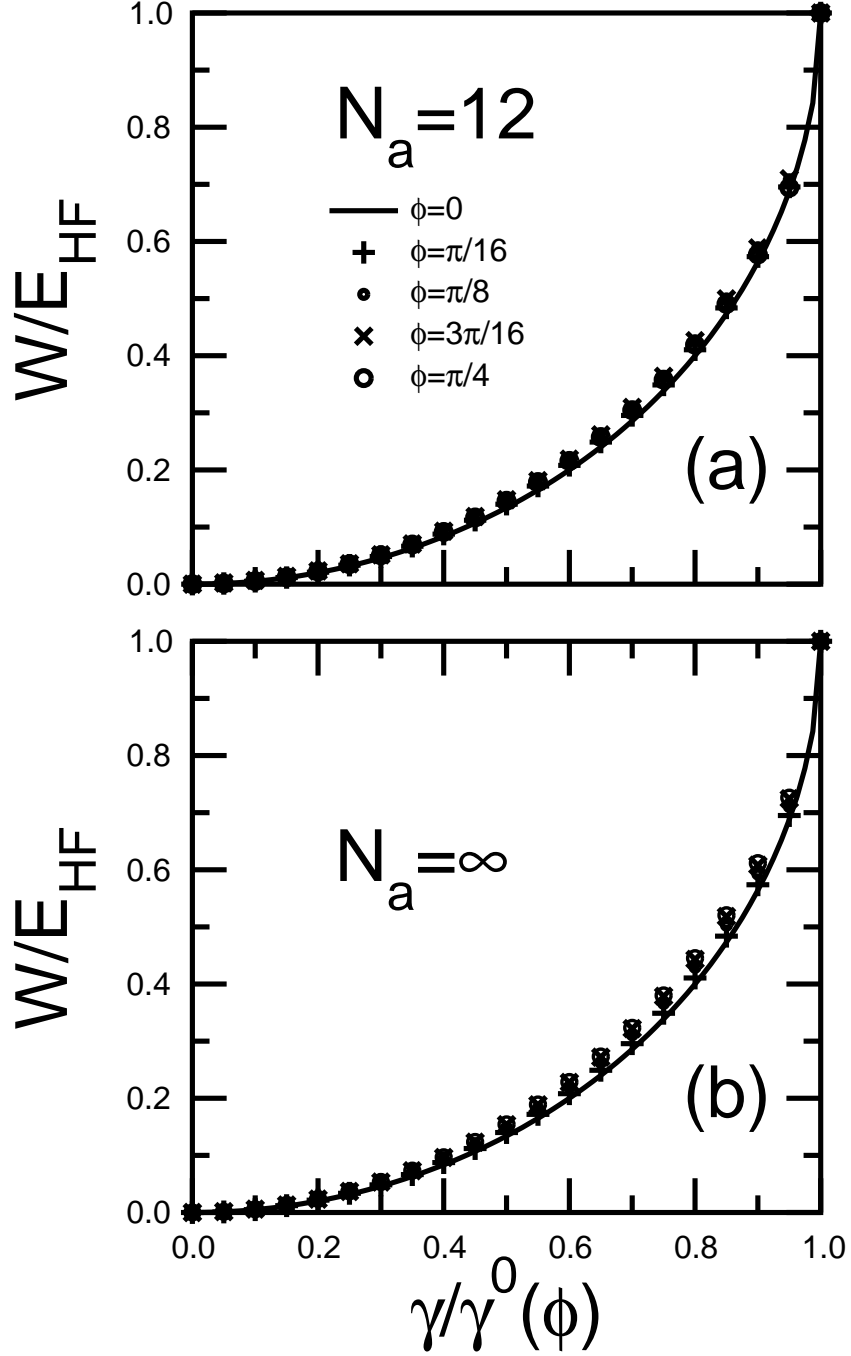


FIG. 3: Interaction-energy W of the 1D Hubbard model as a function of γ/γ^0 for different $\phi = \arctan(\gamma_{12}/\gamma_{23})$. $\gamma = \sqrt{\gamma_{12}^2 + \gamma_{23}^2}$ and $\gamma^0(\phi)$ is the largest representable value of γ for the given ϕ , which corresponds to the uncorrelated limit ($0 \leq \gamma \leq \gamma^0$, see Fig. 1). Results are shown for (a) the $N_a = 12$ site ring and (b) the infinite chain, both at half-band filling.

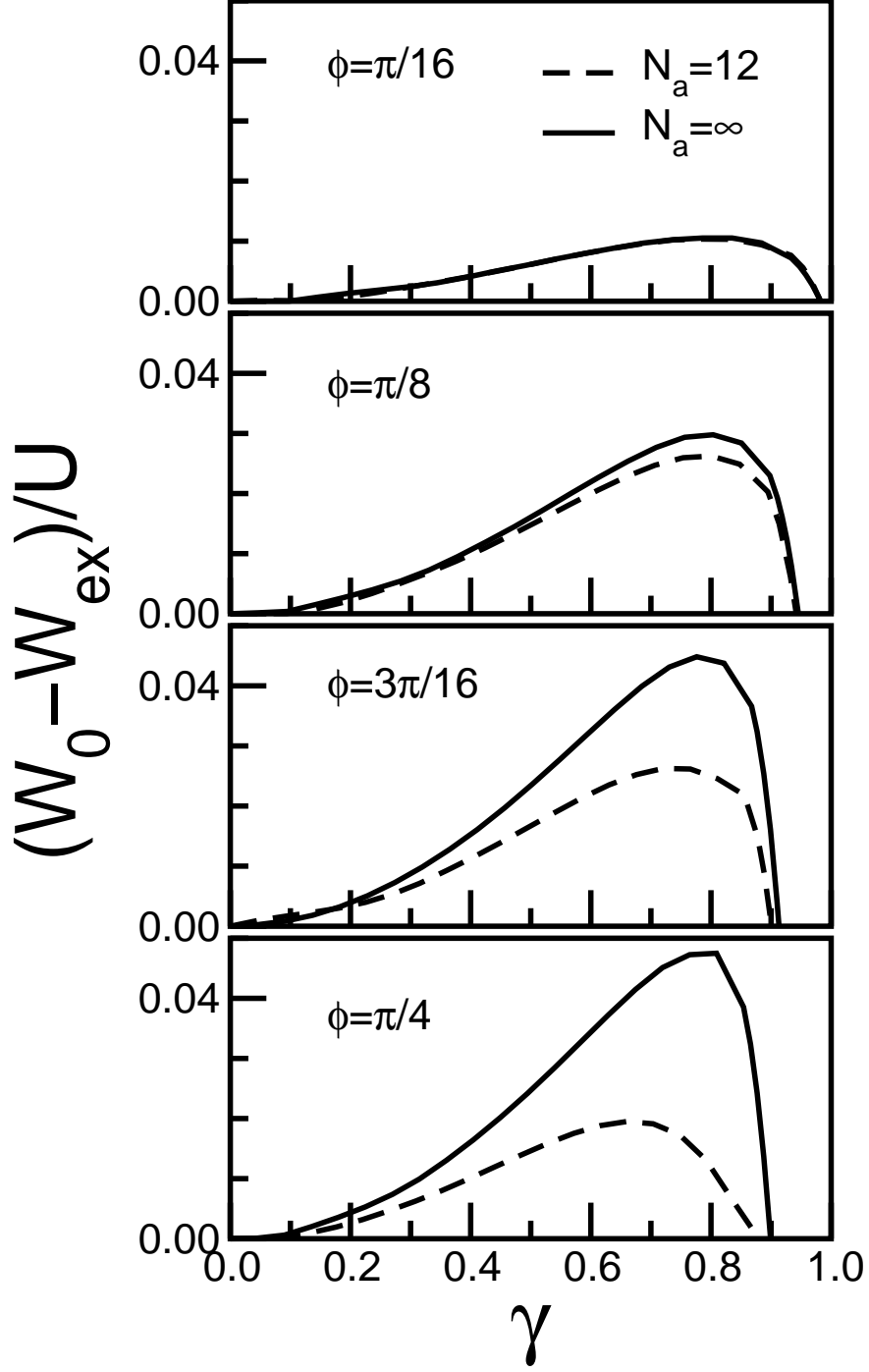


FIG. 4: Comparison between the exact interaction-energy functional W_{ex} of the Hubbard model and the approximation W_0 given by Eq. (21). Results are given for the $N_a = 12$ site ring (dashed) and the infinite chain (solid) as a function of $\gamma = \sqrt{\gamma_{12}^2 + \gamma_{23}^2}$ for different $\phi = \arctan(\gamma_{12}/\gamma_{23})$.

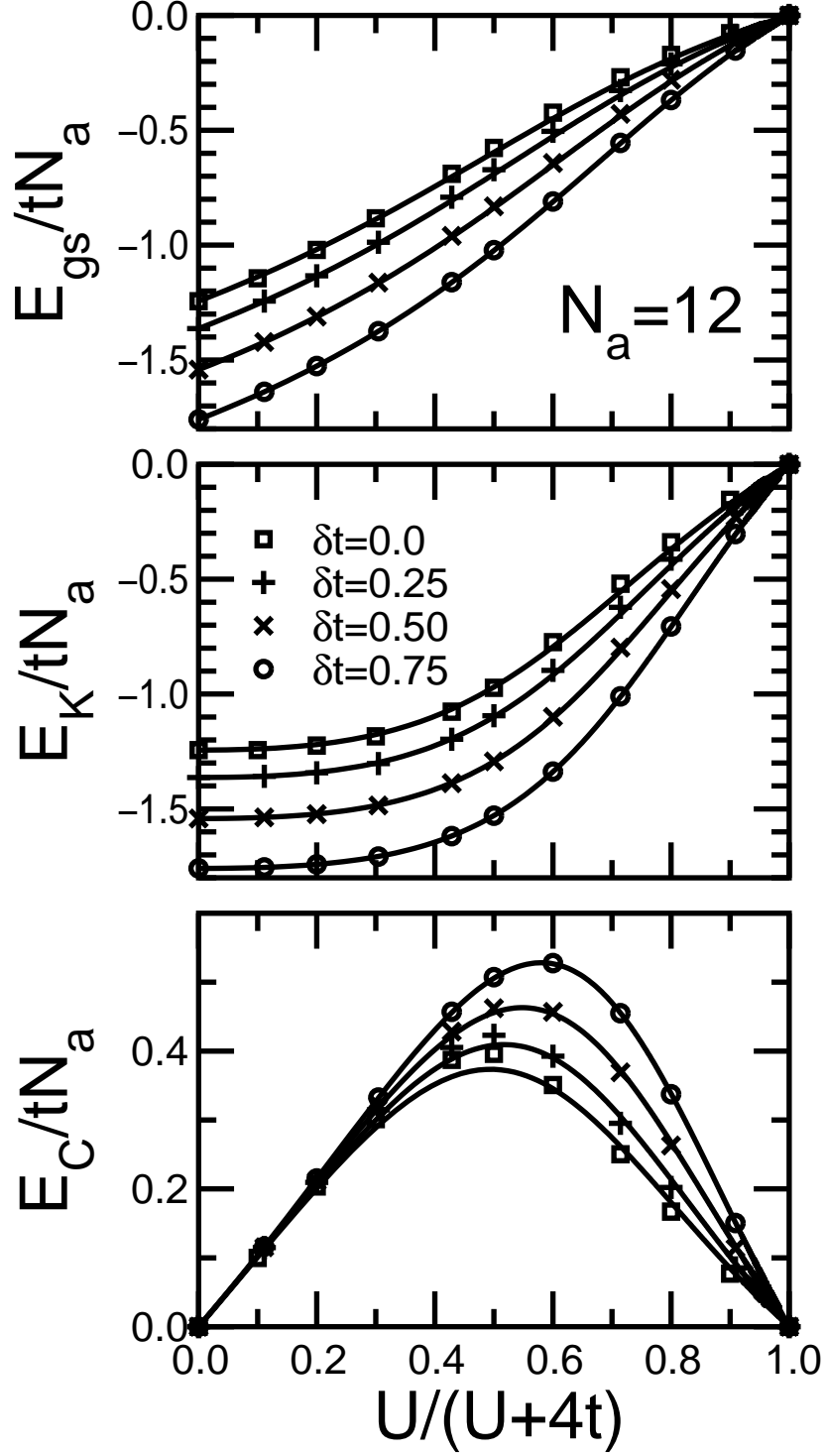


FIG. 5: Ground-state energy $E_{gs} = E_K + E_C$, kinetic energy E_K , and Coulomb energy E_C of dimerized Hubbard rings with hopping integrals $t_{ij} = t(1 \pm \delta t)$, Coulomb interaction U , $N_a = 12$ sites, and $N_e = N_a$ electrons. The symbols are obtained from exact Lanczos diagonalizations²³ and the solid curves correspond to the present lattice density-functional theory.

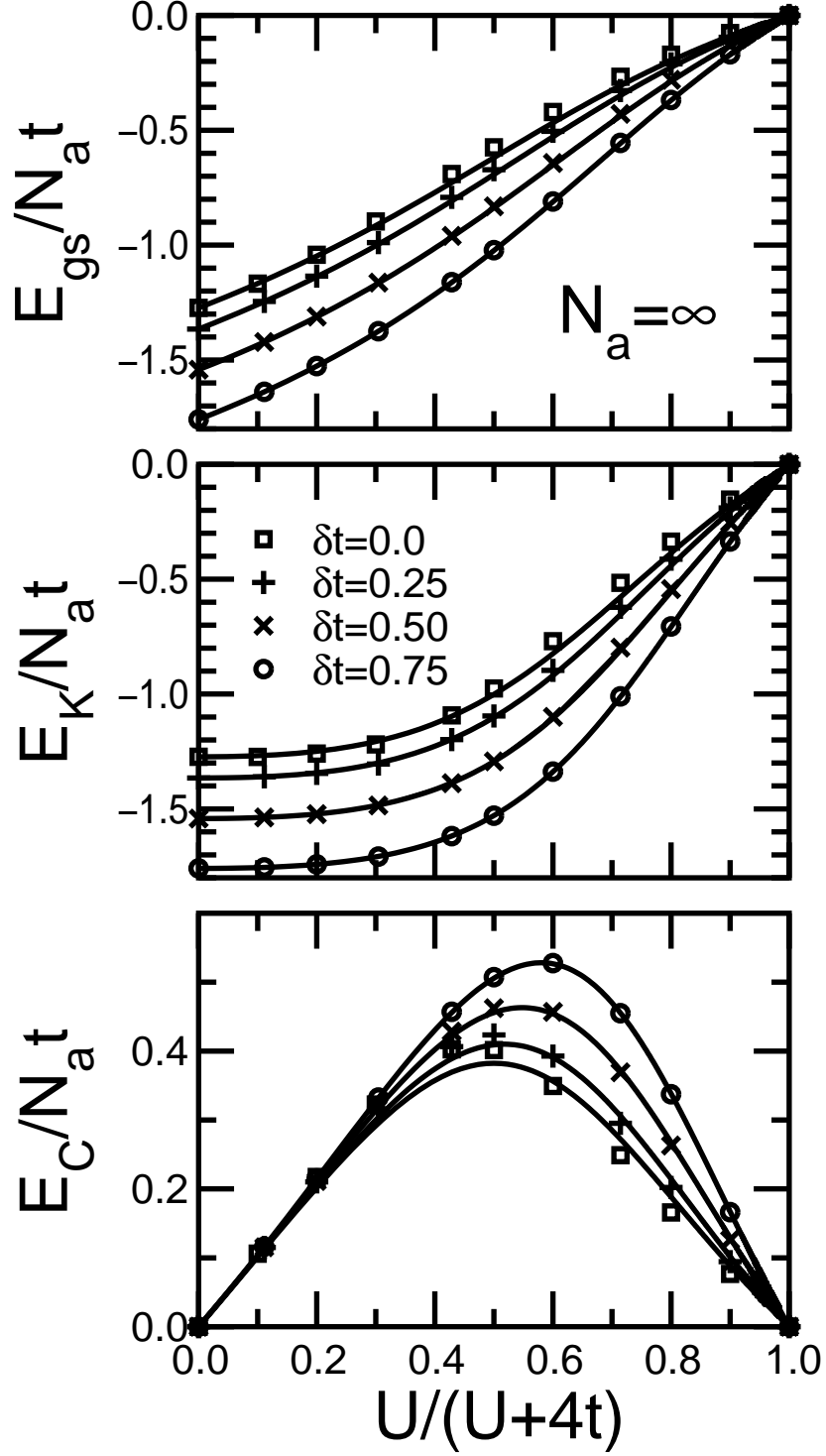


FIG. 6: Ground-state energy $E_{gs} = E_K + E_C$, kinetic energy E_K , and Coulomb energy E_C of dimerized infinite Hubbard chains with hopping integrals $t_{ij} = t(1 \pm \delta t)$. The symbols are obtained using the density-matrix renormalization group method²⁴ and the solid curves correspond to the present lattice density-functional theory (see Fig. 5).

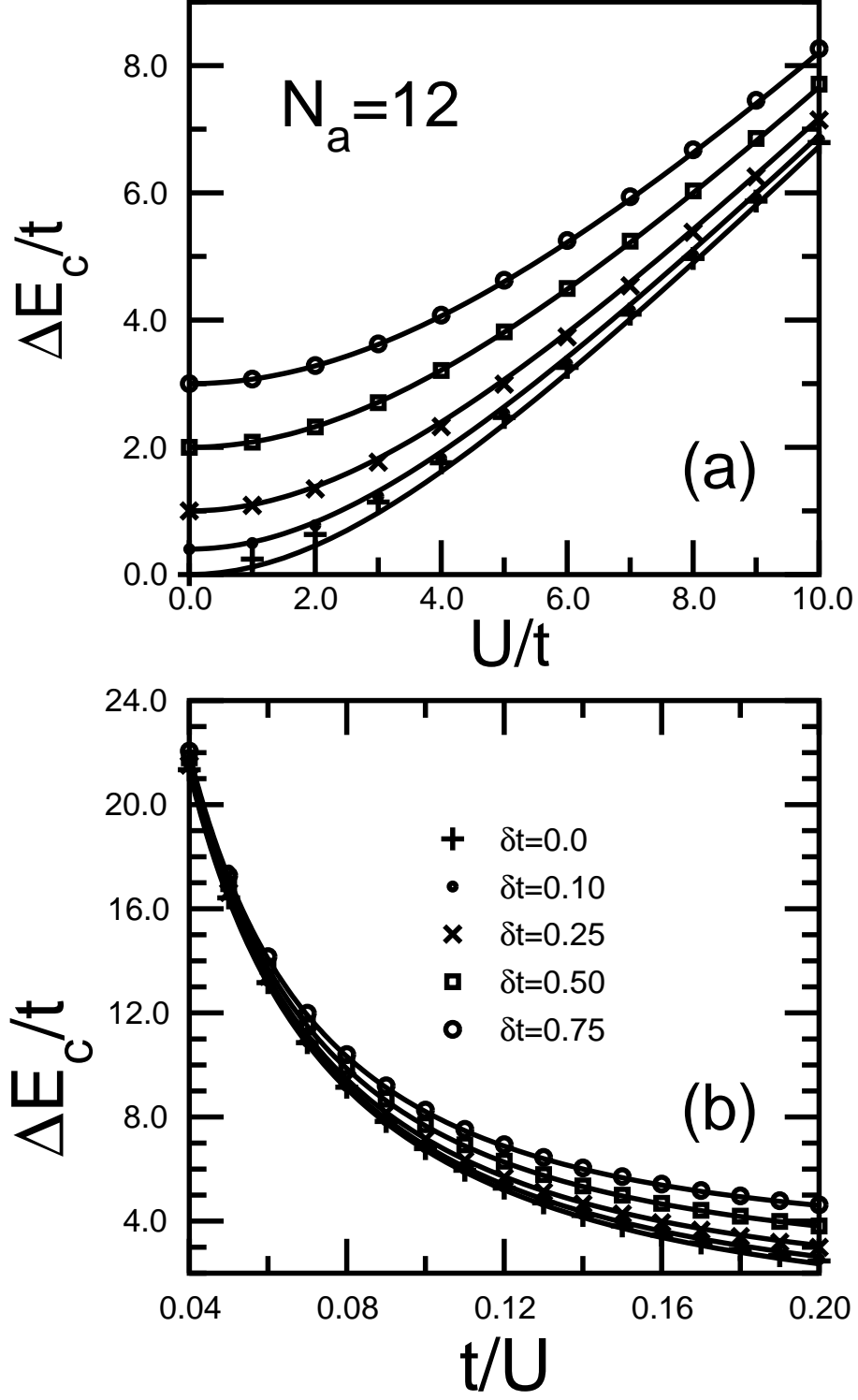


FIG. 7: Charge-excitation gap ΔE_c of dimerized Hubbard rings with $N_a = 12$ sites, hopping integrals $t_{ij} = t(1 \pm \delta t)$, and band filling $n = N_e/N_a = 1$. The symbols refer to exact numerical diagonalizations²³ and the curves to the present lattice density-functional approach.

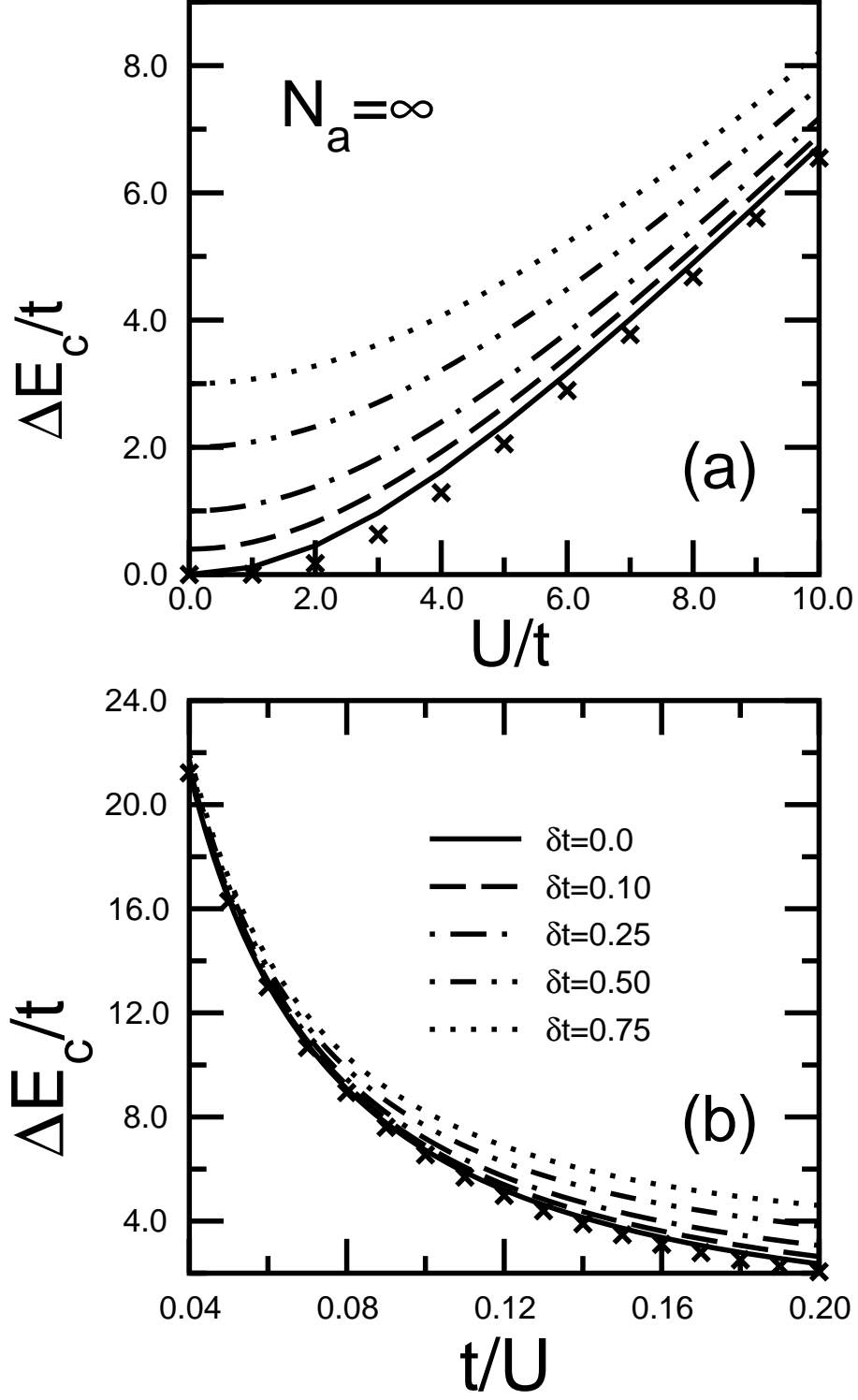


FIG. 8: Charge-excitation gap ΔE_c of dimerized 1D Hubbard chains with hopping integrals $t_{ij} = t(1 \pm \delta t)$ and band filling $n = N_e/N_a = 1$. The crosses refer to exact Bethe-Anstaz results for $\delta t = 0$ (see also Fig. 7).